Heterogeneous Phase Behavior of Solid Carbon Dioxide in Light Hydrocarbons at Cryogenic Temperatures

ROBERT H. JENSEN and FRED KURATA

University of Kansas, Lawrence, Kansas

Solubilities of solid carbon dioxide in liquid ethane, propane, and n-butane were measured from the hydrocarbon triple point or mixture eutectic point to the triple point of carbon dioxide, and an experimental uncertainty was determined for each data point. A eutectic point was discovered in the carbon dioxide–*n*-butane system at approximately 134°K., with a eutectic composition of approximately 0.25 mole % carbon dioxide. A nonlinear least squares analysis was used to fit the binary solubility data and carbon dioxide-methane data from the literature to the Wilson equation for the liquid-phase carbon dioxide activity coefficient. Better agreement with experimental data was obtained by adding two empirical constants to the Wilson equation. This study shows that the Wilson equation is an excellent model for solid carbon dioxide solubility in liquid methane, ethane, propane, and *n*-butane, over the entire composition range, and that the Wilson equation provides a better model than do correlations based on regular solution theory.

The ternary system carbon dioxide-methane-ethane was also studied, and liquid and vapor compositions were measured for each of ten ternary mixtures in solid-liquid-vapor equilibrium. Ternary phase diagrams were constructed, and an empirical correlation was derived for solid carbon dioxide solubility in methane-ethane mixtures above 166°K. An important finding was that solid carbon dioxide is more soluble in some mixtures of methane and ethane than in either of the pure components.

Advances in technology have made cryogenic gas processing both technically and economically attractive, as is shown by the use of modern cryogenic processes such as hydrogen liquefaction, natural gas liquefaction, and the recovery of helium and other low-boiling components from natural gas. However, the full potential of cryogenic processing cannot be realized until reliable cryogenic phase behavior data become as available to plant designers as are data at higher temperatures.

Since carbon dioxide is present as a contaminant in many gases considered for cryogenic processing, the solubility of solid carbon dioxide in liquefied gases must be considered in cryogenic process designs. Failure to account for solid formation could lead to clogged process equipment and resultant plant shutdowns and safety hazards.

Although the removal of carbon dioxide from process gases is normally accomplished at above ambient temperatures, the logic of high-temperature techniques is questionable if the purified gases are to be involved in cryogenic processing. The costs of scrubbing gases at above ambient temperatures are avoided if a cryogenic method of removing carbon dioxide is designed as part of an overall cryogenic scheme.

The purpose of this paper is to provide reliable data and correlations for use in the design of cryogenic processes involving systems of solid carbon dioxide in light hydrocarbons.

SOLUBILITY OF SOLIDS IN LIQUIDS

Solid-liquid equilibria considered in this study are those for which the solid phase is assumed to be pure solute and the liquid phase is a saturated solution of the solute in the solvent. This assumption is justified because the equations derived on the basis of this assumption reliably predict the carbon dioxide solubility. For such a system, Equation (1) is the equation of equilibrium, at constant temperature and pressure, which relates fugacity of the pure solid solute to properties of the liquid mixture (*16*).

$$f_2^S = \gamma_2 \, x_2 \, f_2^L \tag{1}$$

Another relationship which must hold at equilibrium is that the sum of the free energy changes in the hypothetically separate processes of melting the solid to form pure subcooled liquid and mixing the liquid with solvent to the equilibrium concentration must be zero. The free energy of fusion for the melting process may be evaluated from thermodynamic properties of the solute (*10*).

$$-\Delta\overline{F}_2{}^M = \Delta F_2{}^F = \Delta S_2{}^F|_{T_0} \, (T_0 - T) - \Delta C_p (T_0 - T) + T \, \Delta C_p \ln \, (T_0 - T) \tag{2}$$

where C_p is assumed to be independent of temperature. Since subcooled liquid carbon dioxide is a hypothetical fluid, a common simplification of Equation (2) is to remove the terms in ΔC_p, especially at temperatures near the triple point T_0, where the terms tend to cancel. Although temperatures in this study extend far below the triple point, the C_p terms are dropped. Solid-liquid equilibria may therefore be described by Equation (3):

$$-\Delta F_2{}^F = \Delta S_2{}^F|_{T_0} \, (T - T_0) = RT \ln \, (f_2{}^S/f_2{}^L) = RT \ln \, (\gamma_2 \, x_2) = \Delta\overline{F}_2{}^M \tag{3}$$

At this point an assumption must be made regarding the analytical form of the partial molal free energy of mixing $\Delta\overline{F}_2{}^M$. Deviation of this term from ideal solution behavior may be expressed by the excess partial molal free energy $\Delta\overline{F}_2{}^E$. Cheung and Zander (*2*) and Preston and Prausnitz

---

Robert H. Jensen is with Universal Oil Products Company, Riverside, Illinois.

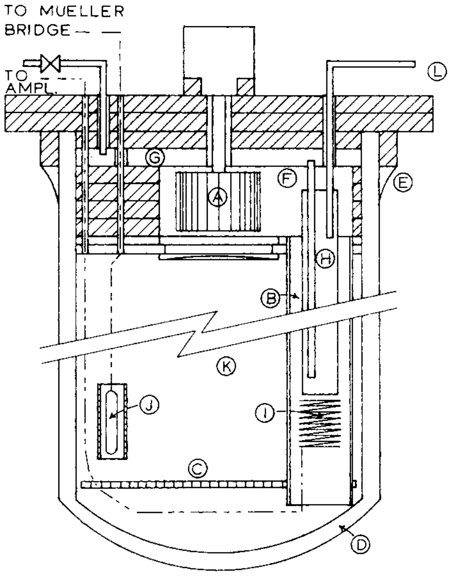

Fig. 1. Controlled-temperature bath.

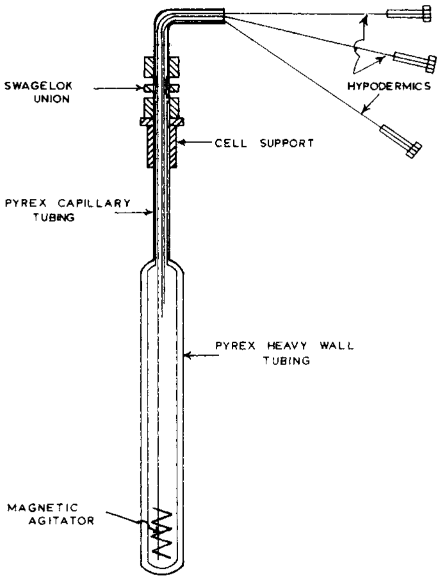

Fig. 2. Equilibrium cell.

(*16*) have used a modification of the Scatchard-Hildebrand equation to describe the excess partial molal free energy. Their equations are based on Hildebrand's regular solution theory (*9*). As an alternative to a regular solution approach, the excess free energy of mixing may be expressed by the Wilson equation, which is based on an extension of the Flory-Huggins equation for athermal mixtures (*20*). The Wilson equation for the excess free energy of mixing for a binary mixture is (*15*)

$$\Delta F^E = RT\,[-x_1 \ln(x_1 + \Lambda_{12}\, x_2) - x_2 \ln(\Lambda_{21}\, x_1 + x_2)] \qquad (4)$$

where

$$\Lambda_{12} \equiv (v_2/v_1) \exp\,[-(\lambda_{12} - \lambda_{11})/RT] \qquad (5)$$

$$\Lambda_{21} \equiv (v_1/v_2) \exp\,[-(\lambda_{12} - \lambda_{22})/RT] \qquad (6)$$

The Wilson parameters, $(\lambda_{ij} - \lambda_{ii})$, with $\lambda_{ij} = \lambda_{ji}$, are empirically determined energy terms which are closely related to the difference in cohesive energy between an *i-j* molecular pair and an *i-i* molecular pair. The expression for the solute partial molal excess free energy of mixing is

$$\Delta \overline{F}_2^E = RT \ln \gamma_2 = RT\,[1 - \ln(x_2 + \Lambda_{21}\, x_1) - x_2/(x_2 + \Lambda_{21}\, x_1) - x_1\, \Lambda_{12}/(x_1 + \Lambda_{12}\, x_2)] \qquad (7)$$

Equations (3) and (7) are combined to find the Wilson equation for solid solubility:

$$\Delta \overline{F}_2^M = \Delta S_2^F|_{T_0}\,(T - T_0) = RT \ln x_2 + RT\,[1 - \ln(x_2 + \Lambda_{21}\, x_1) - x_2/(x_2 + \Lambda_{21}\, x_1) - x_1\, \Lambda_{12}/(x_1 + \Lambda_{12}\, x_2)] \qquad (8)$$

Null (*14*) has applied successfully the Wilson equation to solid-liquid equilibria in high-temperature systems, above 780°K., by using empirical modifications of Equations (5) and (6). Orye and Prausnitz (*15*) have shown that the Wilson equation is an excellent model for the correlation of binary vapor-liquid equilibria data and that it appears to provide a sound basis for the prediction of vapor-liquid equilibria in multicomponent systems.

EXPERIMENTAL PROCEDURE

Apparatus was constructed for this investigation to provide a controlled-temperature environment for a high-pressure glass equilibrium cell in which experimental mixtures were contained and observed (*11*). The controlled-temperature bath is shown schematically in Figure 1. The bath was enclosed in glass Dewar flask (*D*), which had diametrically opposing unsilvered viewing slits. The Dewar was held against the top plate of the bath by spring-tensioned platform, and a rubber sleeve (*E*) provided a leakproof seal between the top of the bath and the Dewar. The bath fluid, air, was circulated by a squirrel-cage blower (*A*) driven by an air motor. Air was drawn up by the blower into the blower housing (*F*) and forced downward through the downcomer tube (*B*) and upward again through perforated plate (*C*). The top of the bath was a sandwich insulation held together by nylon bolts. Liquid nitrogen was the bath refrigerant and entered the system from a pressurized supply Dewar through tube (*L*). The nitrogen passed through heat exchanger (*H*), into heat shield (*G*), and out of the system through a manually adjusted needle valve.

The temperature control system consisted of platinum resistance thermometer (*J*), a Mueller bridge, a null detector, a D. C. amplifier, and nichrome heater (*I*). The difference between the Mueller bridge resistance setting and the thermometer resistance served as an error signal to the null detector, which sent the signal as input to the D. C. amplifier, which provided electrical power to the nichrome heater. Automatic temperature control could be attained in the temperature range 90° to 325°K. by balancing refrigerant flow with the addition of heat. The probable error in a temperature measurement, due to gradients in the bath, was ± 0.15°K.

A 22-cc. Pyrex glass equilibrium cell, pressure tested to 68 atm. and shown in Figure 2, occupied the open area (*K*) of the controlled-temperature bath. The glass capillary cell neck extended out of the bath through a hole in the top insulation and was joined to ¼-in. copper tubing by a Swagelok union. Three 22-gauge hypodermic tubes passed through a silver-soldered seal at the lower end of the copper tubing and into the cell.

Experimental procedure for solubility determinations was first to admit carbon dioxide to the cell through the long inlet hypodermic tube at a bath temperature above the carbon dioxide triple point. Hydrocarbon was next admitted to the cell, which flushed the hypodermic of carbon dioxide, and the bath was cooled to a temperature at which carbon dioxide began to freeze out of solution. The solid-liquid mixture was agitated for 1 hr. before liquid or vapor samples were taken. Carbon dioxide crystals either sank to the bottom of the cell or became electrostatically charged during agitation and were attracted to the cell wall, leaving clear liquid or vapor at the top of the cell for sampling and subsequent analysis by gas chromatog-

Table 1. Purity of Materials

Fluid	Supplier	Grade	Composition, mole %
Carbon dioxide	Matheson Co.	Coleman Instrument	99.99 min. carbon dioxide trace nitrogen
Methane	Phillips Petroleum Co.	Research	99.95 methane 0.05 ethane trace oxygen trace nitrogen
Ethane	Phillips Petroleum Co.	Research	99.99 ethane 0.01 ethylene
Propane	Phillips Petroleum Co.	Research	99.99 propane 0.01 ethane
n-Butane	Phillips Petroleum Co.	Research	99.97 *n*-butane 0.02 isobutane 0.01 butene-2

raphy.

In the analytical procedure sample pressures of 1 atm. or above were required. Since the mixture vapor pressure for a binary system was usually less than 1 atm., the mixture was compressed to a pressure level above 1 atm. so that liquid samples of the desired size could be taken. To verify that samples thus obtained were valid for saturation conditions, the cell was periodically pressurized to above 20 atm., and additional liquid samples were taken. No changes were found in the analyses of these high-pressure samples.

Vapor-phase samples were taken only from the ternary system, for which all vapor pressures were above 8 atm. The cell was filled to approximately one-fifth of its volume with the solid and liquid phases, which left a large volume for vapor sampling. The cell pressure was determined by a previous liquid sampling run, in which only a small vapor space existed in the cell neck.

For vapor pressure measurements, a large vapor space was employed, and a pressure gauge or mercury manometer was connected to a hypodermic at the top of the cell.

The pure components used in this study were received with composition analyses from the suppliers. Before the fluids were used, the analyses were checked by gas chromatography and found to be within the specifications stated in Table 1.

SOLID SOLUBILITY IN BINARY SYSTEMS

Experimental solid carbon dioxide solubility data from this investigation for the systems carbon dioxide-ethane, carbon dioxide-propane, and carbon dioxide–*n*-butane are presented in Tables 2, 3, and 4, respectively. A nonlinear least squares analysis, based on the method of Wolberg (*21*), was used to fit experimental carbon dioxide liquid-phase activity coefficients from each system to the Wilson equation. This procedure was also applied to literature data (*1*, *5*, *8*) for the carbon dioxide-methane system.

An equation for the experimental activity coefficients was obtained from Equation (3):

$$\gamma_2 = \{\exp\,[\Delta S_2^F|_{T_0}\,(T - T_0)/RT]\}/x_2 \qquad (9)$$

The entropy of fusion of carbon dioxide at the triple point $\Delta S_2^F|_{T_0}$ was assumed equal to the value at the melting point, as suggested by Preston and Prausnitz (*16*), and the triple point temperature was taken to be the value used by Cheung and Zander (*2*). Those values, and $R = 1.9872$ cal./(g.-mole)(°K.), were substituted into Equation (9):

$$\gamma_2 = \{\exp\,[4.86\,(T - 216.56)/T]\}/x_2 \qquad (10)$$

Molal volumes of the solvent and solute v_1 and v_2, respectively, were required to compute Λ_{12} and Λ_{21} in Equations (5) and (6). Literature volumetric data for the hydrocarbons were fitted to fourth-order polynomials in

Table 2. Solid Carbon Dioxide Solubility in Liquid Ethane

Temperature, °K.	Experimental x_2^{exp} mole %	σ_{x_2} mole %
213.2	91.08	0.21
209.3	72.84	0.15
205.4	48.90	0.29
199.8	28.43	0.52
194.3	18.13	0.53
188.7	11.68	0.42
183.2	8.01	0.09
177.6	6.07	0.09
172.0	4.15	0.05
166.5	2.90	0.01
160.9	2.01	0.01
155.4	1.34	0.01
152.6	1.12	0.01
144.3	0.588	0.01
135.9	0.305	0.01
134.3	0.277	0.01
127.6	0.137	0.003
116.5	0.043	0.004
105.4	0.013	0.003

Table 3. Solid Carbon Dioxide Solubility in Liquid Propane

Temperature, °K.	Experimental x_2^{exp} mole %	σ_{x_2} mole %
212.0	82.74	1.09
210.9	75.60	1.09
208.4	53.16	0.25
205.9	38.96	0.55
204.8	35.10	0.39
199.8	21.81	0.14
198.7	20.44	0.40
193.4	13.31	0.25
188.7	9.85	0.33
183.2	7.29	0.14
177.6	5.35	0.05
172.0	3.79	0.05
160.9	1.99	0.03
158.2	1.70	0.05
155.4	1.40	0.03
149.8	0.908	0.05
144.3	0.542	0.02
138.7	0.343	0.02
127.6	0.126	0.003
124.8	0.096	0.004
122.0	0.073	0.005
108.2	0.025	0.005

Table 4. Solid Carbon Dioxide Solubility in Liquid n-Butane

Temperature, °K.	Experimental $x_2^{\exp}$ mole %	σ_{x_2} mole %
213.2	85.50	0.18
210.9	61.86	2.03
208.2	37.42	0.89
205.4	30.27	0.62
199.8	17.53	0.39
188.7	10.50	0.82
183.2	7.01	0.05
177.6	5.22	0.06
172.0	3.71	0.10
166.5	2.55	0.02
160.9	1.82	0.06
155.4	1.28	0.02
149.8	0.896	0.02
144.3	0.581	0.01
138.7	0.403	0.01
135.9	0.299	0.01
135.4	0.268	0.01
134.6	0.154	0.006
134.5	0.028	0.004

Table 5. Wilson Parameters ($\lambda_{ij} - \lambda_{ii}$) for Solid Carbon Dioxide Solubility in Binary Systems

System	$\lambda_{12} - \lambda_{11}$ cal./g.-mole	$\lambda_{12} - \lambda_{22}$ cal./g.-mole
CO_2-CH_4	521.05	661.32
CO_2-C_2H_6	271.35	693.48
CO_2-C_3H_8	342.43	753.18
CO_2-n-C_4H_{10}	448.95	795.08

Table 6. Modified Wilson Equation Parameters for Solid Carbon Dioxide Solubility in Binary Systems

System	α_1 cal./g.-mole	$\alpha_2 \times 10^{-3}$ (cal./g.-mole)^2	β_1 cal./g.-mole	$\beta_2 \times 10^{-3}$ (cal./g.-mole)^2
CO_2-CH_4	739.99	−100.80	667.33	4.4382
CO_2-C_2H_6	766.55	−183.24	329.86	124.48
CO_2-C_3H_8	671.88	−97.946	517.34	71.864
CO_2-n-C_4H_{10}	1044.4	−238.45	680.45	43.940

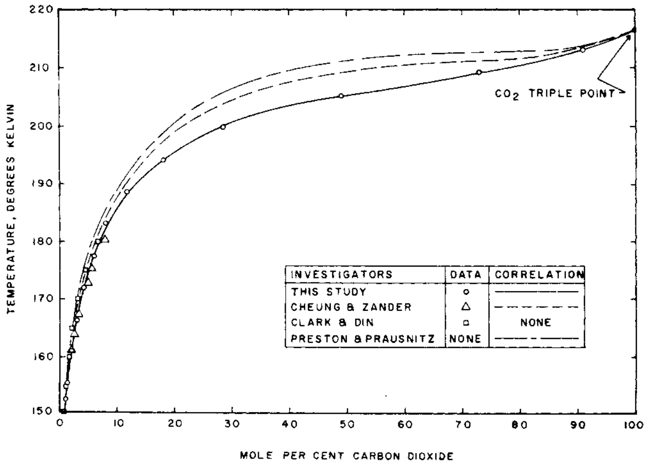

Fig. 3. Solid carbon dioxide solubility in liquid ethane; 0 to 100% carbon dioxide.

temperature by the method of linear least squares (*21*). Molal volumes of subcooled liquid carbon dioxide were computed at 27 temperatures from 91° to 216°K. by Lydersen's method (*18*), using Din's triple point volume, 0.8490 cc./g. (*6*) as the reference volume. The resulting carbon dioxide liquid molal volumes were also fitted to a fourth-order polynomial[*]:

$$v_i = \Sigma^4{}_{k=0}\, D_{ik}\, T^k \tag{11}$$

The nonlinear least squares analysis found values of ($\lambda_{12} - \lambda_{11}$) and ($\lambda_{12} - \lambda_{22}$) which minimized the weighted sum of the squares of the differences between observed and calculated variables in the Wilson equation. Estimates of experimental uncertainties for the dependent variable $\ln \gamma_2$ and the two independent variables x_2 and T were required to properly weight each data point in each binary system. Uncertainty in an experimental mole fraction σ_{x_2} was taken to be the larger of two quantities. The first quantity was the standard deviation of actual chromatographic standard mixture mole fractions from mole fractions computed from least square calibration polynomials, which were found by analyzing standard mixtures each day a run was made. The second quantity was the standard deviation of the average experimental mole fraction from all of the samples analyzed at the bath temperature in question. Uncertainties in mole fractions determined by this procedure are listed in Tables 2 to 4. Uncertainty in $\ln \gamma_2$ was estimated from Equation (12) for each data point:

$$\sigma_{\ln \gamma_2} \cong \sigma_{x_2}/x_2 \tag{12}$$

The uncertainty in each temperature measurement was arbitrarily set equal to 0.2°K.

For the carbon dioxide-methane literature data, σ_{x_2} was taken to be 2% of the reported mole percent, estimates of $\sigma_{\ln \gamma_2}$ were calculated from Equation (12), and uncertainty in temperature was assumed to be 0.02°K. for each data point.

Least square values of the Wilson parameters ($\lambda_{12} - \lambda_{11}$) and ($\lambda_{12} - \lambda_{22}$) are presented in Table 5 for each binary system. Better agreement with experimental data was obtained by adding two empirical constants to Equations (5) and (6):

$$\Lambda_{12} \equiv (v_2/v_1) \exp\left[-\alpha_1/RT - \alpha_2/(RT)^2\right] \tag{13}$$

$$\Lambda_{21} \equiv (v_1/v_2) \exp\left[-\beta_1/RT - \beta_2/(RT)^2\right] \tag{14}$$

Least square values of α_1, α_2, β_1, and β_2 are given in Table 6 for each binary system.

The calculation of solid carbon dioxide solubility with the Wilson equation is a trial and error procedure.[†] At a given temperature Λ_{12} and Λ_{21} are first calculated from Equations (5) and (6) or from Equations (13) and (14). An initial guess, 1, for example, is made for γ_2, and x_2 is computed from Equation (10). γ_2 is then calculated from Equation (7) and compared with the initial guess. If the two values do not agree, the new value of γ_2 is used to recalculate x_2, and the procedure is repeated until con-

---

[*] Least square constant D_{ik} and standard deviation σ_v of calculated volumes from literature have been deposited as document 01321 with the ASIS National Auxiliary Publications Service, c/o CCM Information Sciences, Inc., 909 Third Ave., New York 10022 and may be obtained for $2.00 for microfiche or $6.50 for photocopies.

[†] Solubilities calculated from the original Wilson equation and from the modification given by Equations (13) and (14) have been filed with the ASIS. Numerical comparisons with the experimental data are given for each system, including carbon dioxide-methane.

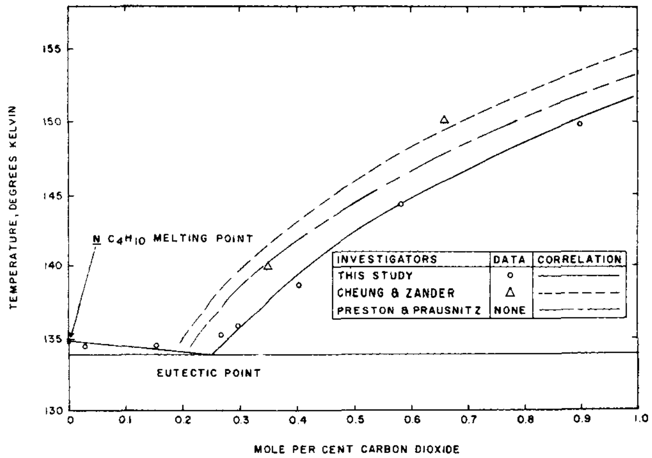

Fig. 4. Solid carbon dioxide solubility in liquid *n*-butane; 0 to 1.0% carbon dioxide.

vergence is obtained. A change in the computational procedure is made for the carbon dioxide-methane system at temperatures above 180°K. Since Equation (11) becomes invalid as the methane critical temperature 191.1°K. is approached, the ratio v_2/v_1 in Equations (5), (6), (13), and (14) is assumed equal to the ratio at 180°K. for temperatures greater than 180°K.

The binary system carbon dioxide-ethane is shown graphically in Figure 3 over the complete composition range of 0 to 100 mole % carbon dioxide. Data and correlations of other investigators are included on the graph for comparison with the data and four-parameter Wilson equation correlation of this study. This figure indicates that the correlation of this study is in good agreement with experimental data from the triple point of ethane to the triple point of carbon dioxide. The other correlations are fairly reliable for low carbon dioxide solubilities, and they could probably be improved by using the data of this study to find improved values of required empirical constants. The same conclusion is drawn for the other three binary systems after the data and correlations are compared.

A eutectic point was discovered in the carbon dioxide–*n*-butane system at 134°K., ±0.5°K., with a eutectic composition of 0.25 mole % carbon dioxide, ±0.02 mole %. The point was graphically determined, as shown in Figure 4, by the intersection of the four-parameter Wilson equation correlation with the best straight line drawn through the *n*-butane melting point and between the two data points to the left of the eutectic. The eutectic was visually verified by the observation of slender, needlelike crystals, assumed to be *n*-butane, below the *n*-butane freezing point, in the two mixtures containing less than 0.25 mole % carbon dioxide. Carbon dioxide crystals were shaped like tiny wafers and were found at higher compositions. To verify that impurities in the *n*-butane were not causing a false eutectic, the freezing point of pure *n*-butane was experimentally measured and was found to agree to within experimental accuracy with 134.80°K., the value specified by Phillips Petroleum Company. Because of the eutectic point, the carbon dioxide–*n*-butane Wilson parameters should not be used for carbon dioxide compositions less than 0.25 mole %.

Table 7. Solid-Liquid-Vapor Phase Equilibrium Data for the Carbon Dioxide-Methane-Ethane System

Temperture, °K.	Pressure, atm.	Liquid composition, mole %		Vapor composition, mole %	
		CO_2	C_2H_6	CO_2	C_2H_6
208.2	18.34	63.61	20.86	18.89	8.87
208.2	28.46	64.46	11.15	14.21	4.27
205.4	19.15	49.80	28.66	15.67	9.11
205.4	30.09	47.53	15.67	11.68	4.19
199.8	18.75	31.88	38.78	9.14	8.32
199.8	29.68	29.08	21.96	6.75	4.23
183.2	13.98	10.15	51.22	2.97	5.57
183.2	22.49	9.14	27.22	1.92	2.19
166.5	8.86	3.84	55.94	1.05	3.20
166.5	13.64	3.36	29.32	0.87	1.46

Orye and Prausnitz (*15*) have shown that heat of mixing can be estimated from the Wilson equation by utilizing the exact relation

$$\Delta H^M = -T^2 \left[\partial(\Delta F^E/T)/\partial T\right]_{P,x} \qquad (15)$$

If $(\lambda_{12} - \lambda_{11})$ and $(\lambda_{12} - \lambda_{22})$ are assumed to be independent of temperature, the heat of mixing for a binary solution is

$$\begin{aligned}\Delta H^M = {} & x_1\, x_2\, \Lambda_{12}(\lambda_{12} - \lambda_{11})/(x_1 + \Lambda_{12}\, x_2) \\ & + x_1\, x_2\, \Lambda_{21}(\lambda_{12} - \lambda_{22})/(x_2 + \Lambda_{21}\, x_1) \\ & + x_1\, x_2\, RT^2 \left[\Lambda_{12}/(x_1 + \Lambda_{12}\, x_2) - \Lambda_{21}/(x_2 + \Lambda_{21}\, x_1)\right] \\ & \left[(dv_2/dT)/v_2 - (dv_1/dT)/v_1\right] \qquad (16)\end{aligned}$$

If Equations (13) and (14) are used to compute Λ_{12} and Λ_{21}, respectively, the heat of mixing becomes

$$\begin{aligned}\Delta H^M = {} & x_1\, x_2\, (\alpha_1 + \alpha_2/RT)/(x_1 + \Lambda_{12}\, x_2) \\ & + x_1\, x_2\, (\beta_1 + \beta_2/RT)/(x_2 + \Lambda_{21}\, x_1) \\ & + x_1\, x_2\, RT^2 \left[\Lambda_{12}/(x_1 + \Lambda_{12}\, x_2) - \Lambda_{21}/(x_2 + \Lambda_{21}\, x_1)\right] \\ & \left[(dv_2/dT)/v_2 - (dv_1/dT)/v_1\right] \qquad (17)\end{aligned}$$

Heats of mixing computed from Equation (17) are shown in Figure 5. The ratios $(dv_2/dT)/v_2$ and $(dv_1/dT)/v_1$ for the carbon dioxide-methane system were assumed to equal the ratios at 180°K. for temperatures greater than 180°K. The fact that heats computed from Equations (16) and (17) are for mixing hypothetical subcooled liquid carbon dioxide with a liquid hydrocarbon should be remembered when using the equations. For the carbon dioxide-methane system above 191.1°K., the heat computed is for mixing hypothetical subcooled liquid carbon

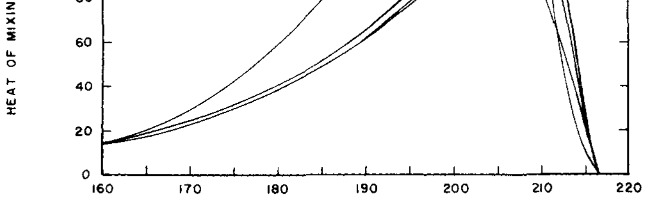

Fig. 5. Heats of mixing for saturated solutions of carbon dioxide in light hydrocarbons; computed from modified Wilson equation.

dioxide with hypothetical supercritical liquid methane. The accuracy of calculated heats of mixing will not be known until experimental enthalpy data become available.

CARBON DIOXIDE-METHANE-ETHANE SYSTEM

Equilibrium temperatures and pressures and liquid-vapor compositions for ten carbon dioxide-methane-ethane mixtures in solid-liquid-vapor equilibrium are presented in Table 7. A three-component, three-phase system at equilibrium possesses two degrees of freedom, and fixing the temperature and pressure determines the state of the system. The liquid and vapor compositions for each mixture in Table 7 are therefore unique points on a ternary phase diagram at constant temperature and pressure.

Figure 6 is a ternary phase diagram on triangular coordinates at 199.8°K. and at 18.75 atm. In constructing the diagram, binary end points were required. For the carbon dioxide-ethane binary, solid-liquid equilibrium points were taken from this study, assuming negligible change in solubility with pressure. Carbon dioxide-methane solid-vapor equilibrium points were graphically interpolated or extrapolated from the results of Donnelly and Katz (*8*) and Davis et al. (*5*). The vapor-liquid equilibrium data of Price and Kobayashi (*17*) were interpolated to obtain the methane-ethane binary end points. Other phase diagrams can be constructed by combining the remaining data in Table 7 with literature data (*11*).

Figure 7 is a ternary diagram showing liquid compositions from Table 7 connected isothermally with the liquid compositions of the two carbon dioxide-hydrocarbon binary systems, each point on the diagram representing a different equilibrium pressure. The diagram illustrates the finding that solid carbon dioxide is more soluble in mixtures of methane and ethane than in either of the pure components, at least over a 40°K. temperature range. Knowledge of this behavior could be very useful in the design of cryogenic processes to remove carbon dioxide from natural gas.

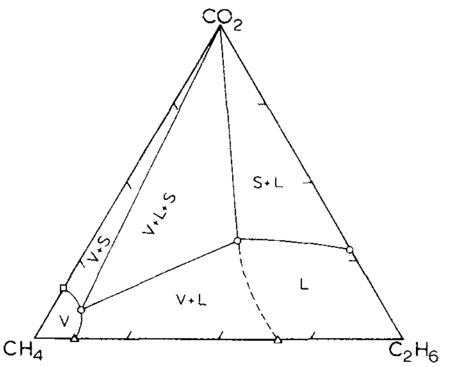

Fig. 6. Carbon dioxide-methane-ethane phase diagram at 199.8°K. and 18.75 atm.

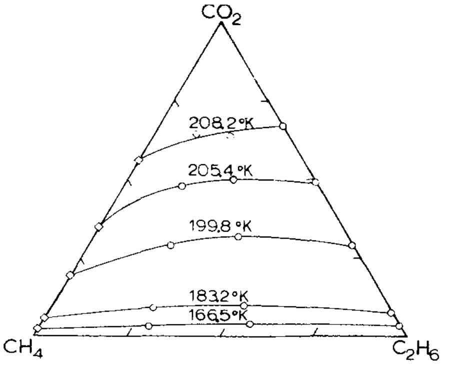

Fig. 7. Liquid-phase compositions for solid-liquid-vapor equilibria in the carbon dioxide-methane-ethane system.

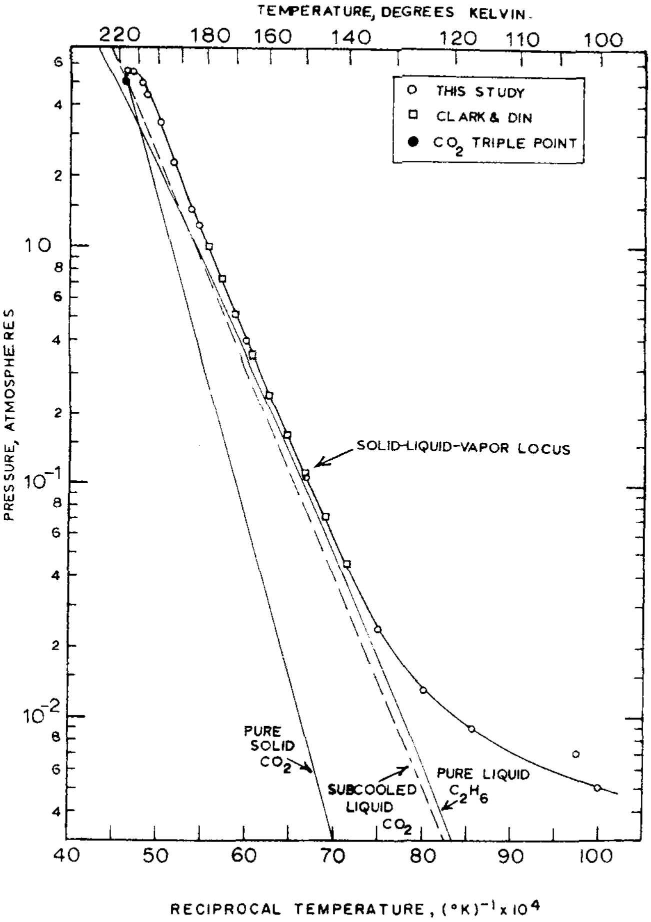

Fig. 8. Vapor pressures of saturated solutions of solid carbon dioxide in liquid ethane and of the pure components.

To predict carbon dioxide solubility in methane-ethane mixtures at an intermediate temperature T in Figure 7, the following equation is presented:

$$x_2 = (1-\theta)x_2^{CH_4} + \theta\, x_2^{C_2H_6} + \theta\,(1-\theta)\,(\epsilon_1 + \epsilon_2\,\theta) \tag{18}$$

where θ is mole fraction ethane, on a carbon dioxide-free basis, in the liquid phase of the ternary system at equilibrium at temperature T; $x_2^{CH_4}$ and $x_2^{C_2H_6}$ are mole fractions carbon dioxide in the carbon dioxide-methane and carbon dioxide-ethane binary systems in solid-liquid-vapor equilibrium at temperature T; and ϵ_1 and ϵ_2 are empirical functions of temperature. Inspection of Equation (18) reveals that if $\theta = 0$ or $\theta = 1$, the equation reduces to solid carbon dioxide solubility in a binary system. The binary solubilities are the end points of the curves in Figure 7, and if ϵ_1 and ϵ_2 are equal to zero, the equation is simply the molal average of the binary solubilities. The effect of ϵ_1 on the equation is to increase or decrease the height of an isotherm, and the effect of ϵ_2 is to shift the maximum or minimum point of the isotherm.

Empirical constants ϵ_1 and ϵ_2 were computed for each isotherm in Figure 7 by substituting experimental data points into Equation (18) and solving for the constants. At 208.2°K. ternary points were taken off the smooth curve drawn through the data. The resulting constants are given in Table 8.

If temperature and θ are specified, solid carbon dioxide

TABLE 8. EMPIRICAL CONSTANTS

Temperature, °K.	ϵ_1	ϵ_2
208.2	0.202	−0.151
205.4	0.506	−0.410
199.8	0.369	−0.109
183.2	0.137	−0.0122
166.5	0.0233	0.0368

TABLE 9. VAPOR PRESSURE OF SATURATED SOLUTIONS OF SOLID CARBON DIOXIDE IN LIQUID ETHANE

Temperature, °K.	Pressure, atm.
214.8	5.59
212.6	5.59
208.2	5.04
205.4	4.47
199.8	3.34
193.2	2.28
185.9	1.48
183.2	1.24
166.5	0.393
149.8	0.107
133.2	0.024
124.8	0.013
116.5	0.009
102.6	0.007
99.8	0.005

TABLE 10. VAPOR PRESSURES OF SATURATED SOLUTIONS OF SOLID CARBON DIOXIDE IN LIQUID PROPANE

Temperature, °K.	Pressure, atm.
213.7	4.43
208.2	3.16
205.4	2.55
199.8	1.70
191.5	0.872
183.2	0.445
174.8	0.194
166.5	0.084
158.2	0.038
149.8	0.016
141.5	0.009

TABLE 11. VAPOR PRESSURES OF SATURATED SOLUTIONS OF SOLID CARBON DIOXIDE IN LIQUID *n*-BUTANE

Temperature, °K.	Pressure, atm.
210.9	3.51
208.2	2.86
202.6	1.92
199.8	1.29
191.4	0.736
183.2	0.365
174.8	0.150
166.5	0.059
158.2	0.023
149.8	0.013
149.8	0.011
141.5	0.008

solubility in a methane-ethane mixture above 166°K. can be calculated from Equation (18). For the calculation, $x_2^{CH_4}$ and $x_2^{C_2H_6}$ are found from the correlations for binary solubility, and values of ϵ_1 and ϵ_2 are taken from plots of ϵ_1 and ϵ_2 versus temperature. The required plots can be obtained from the data in Table 8.

This study did not extend to the prediction of solid carbon dioxide solubility in methane-ethane mixtures with the generalized form of the Wilson equation, although it is theoretically possible to compute ternary data using binary Wilson parameters (*15*). Further work in this area is being conducted at the University of Kansas.

VAPOR PRESSURES OF BINARY SYSTEMS

Experimental vapor pressures for the solid-liquid-vapor binary systems studied in this investigation are presented in Tables 9 to 11. Pressures less than 2.6 atm. were measured on a mercury manometer to ±0.0015 atm., and higher pressures were read on a pressure gauge to ±0.03 atm. The carbon dioxide-ethane data are also shown graphically in Figure 8. Vapor pressures of pure ethane (*22*), pure solid carbon dioxide (*6*), and pure subcooled liquid carbon dioxide (*3*) are included on the plot.

The carbon dioxide-ethane system shows marked positive deviation from Raoult's law, the mixture vapor pressure being greater than the vapor pressure of either pure component. This is in agreement with the results of Clark and Din (*4*), who state that the system deviates from ideality to the extent of forming a low-boiling azeotrope. Figure 8 also indicates a maximum in the vapor pressure curve above the carbon dioxide triple point. This phenomenon was reproduced experimentally several times, and the literature triple point pressure, 5.11 atm. (*6*), was experimentally duplicated to ensure that there were no significant impurities in the carbon dioxide.

At a pressure of approximately 0.01 atm., the solid-liquid-vapor saturation pressures begin to curve away from the pure hydrocarbon vapor pressure loci for all three binary systems. This suggests that each system may have a solid carbon dioxide-vapor-liquid-solid hydrocarbon

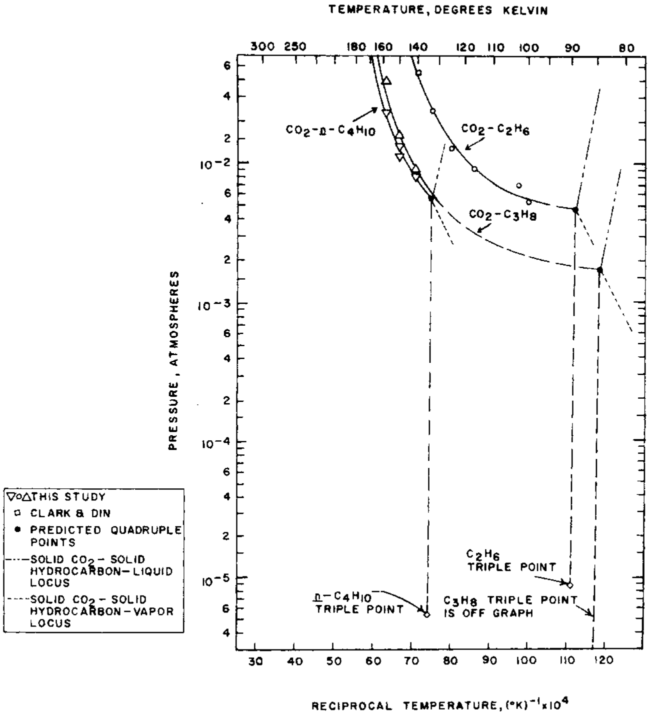

Fig. 9. Predicted quadruple points for the binary systems.

TABLE 12. PREDICTED QUADRUPLE POINTS

System	Temperature, °K.	Pressure, atm.
CO_2-C_2H_6	89	4.7×10^{-3}
CO_2-C_3H_8	85	1.7×10^{-3}
CO_2-C_4H_{10}	134	5.6×10^{-3}

quadruple point at some temperature lower than the hydrocarbon triple point temperature. Limitations of the apparatus prevented an experimental investigation to test the quadruple point hypothesis. However, quadruple point temperatures were estimated to be approximately equal to the hydrocarbon triple point temperatures, and quadruple point pressures were obtained by extrapolating the solid carbon dioxide-liquid-vapor saturation pressure curves to meet solid hydrocarbon-liquid-vapor loci extending up from the hydrocarbon triple points, as shown in Figure 9. Predicted quadruple point conditions are given in Table 12.

CONCLUSIONS

The solid solubility data reported for the carbon dioxide-ethane, carbon dioxide-propane, and carbon dioxide–*n*-butane systems greatly increase the amount of data available for these systems and extend over the previously unexamined composition range 8 to 100 mole % carbon dioxide. The Wilson equation is an excellent model for solid carbon dioxide solubilities in light hydrocarbons over the entire composition range.

The ternary mixture data provide a basis for correlating the phase equilibria of multicomponents systems, and the empirical correlation derived for solid carbon dioxide solubility in methane-ethane mixtures is reliable from 166°K. to the triple point of carbon dioxide.

Vapor pressure measurements confirm that the carbon dioxide-ethane system shows a marked positive deviation from Raoult's Law. Examination of the vapor pressure data leads to the hypothesis that quadruple points exist for the three binary systems studied.

The data and correlations resulting from this investigation will be valuable in the design of cryogenic processes to remove carbon dioxide from light hydrocarbon systems.

ACKNOWLEDGMENT

The authors gratefully acknowledge the National Science Foundation for funds furnished through NSF Grants GK-705 and GK-4193. The University of Kansas Computation Center is also acknowledged for the use of their facilities.

Phillips Petroleum Company donated the research grade hydrocarbons used in this study.

NOTATION

ΔC_p = liquid-solid molal specific heat difference, cal./(g.-mole) (°K.)
D_{ik} = least square constant for molal volume, cc./(g.-mole) (°K.^{k})
ΔF = free energy change, cal./g.-mole
$\Delta \bar{F}$ = partial molal free energy change, cal./g.-mole
f = fugacity
ΔH = enthalpy change, cal./g.-mole
P = pressure, atm.
R = gas law constant, cal./(g.-mole) (°K.)
ΔS = entropy change, cal./(g.-mole) (°K.)
T = temperature, °K.
v = molal liquid volume, cc./g.-mole
x = liquid-phase mole fraction

Greek Letters

α_1, α_2 = empirical constants in Equation (23)
β_1, β_2 = empirical constants in Equation (24)
γ = liquid-phase activity coefficient
ϵ_1, ϵ_2 = empirical functions of temperature
θ = mole fraction ethane, on a carbon dioxide-free basis, in liquid phase of carbon dioxide-methane-ethane system in solid-liquid-vapor equilibrium
Λ_{ij} = temperature-dependent Wilson parameter
$(\lambda_{ij} - \lambda_{ii})$ temperature-independent Wilson parameter, cal./g.-mole
σ = uncertainty or standard deviation in an experimental measurement

Superscripts

CH_4 = carbon dioxide-methane system
C_2H_6 = carbon dioxide-ethane system
E = excess
F = fusion
L = pure subcooled liquid
M = mixing
S = solid

Subscripts

0 = triple point
1 = solvent
2 = solute
i, j = components in solution

LITERATURE CITED

1. Brewer, J., and Fred Kurata, *AIChE J.*, **4**, (3), 317 (1958).
2. Cheung, H., and E. H. Zander, *Chem. Eng. Symp. Ser. No. (88)*, **64**, 34 (1968).
3. Clark, A. M., and F. Din, *Trans. Faraday Soc.*, **46**, 901 (1950).
4. ———, *Discussions Faraday Soc.*, **15**, 202 (1953).
5. Davis, J. A., N. Rodewald, and Fred Kurata, *AIChE J.*, **8**, (4), 537 (1962).
6. Din, F., "Thermodynamic Functions of Gases," Vol. 1, Butterworths, London (1956).
7. *Ibid.*, Vol. 3 (1961).
8. Donnelly, H. G., and D. L. Katz, *Ind. Eng. Chem.*, **46**, 511 (1954).
9. Hildebrand, J. H., and R. L. Scott, "Regular Solutions," Prentice-Hall, Englewood Cliffs, N. J., (1962).
10. ———, "The Solubility of Nonelectrolytes," 3rd edit., Reinhold, New York (1950).
11. Jensen, R. H., Ph.D. thesis, Univ. Kansas, Lawrence (1969).
12. Lewis, G. N., M. Randall, K. S. Pitzer, and L. Brewer, "Thermodynamics," 2nd edit., McGraw-Hill, New York (1961).
13. Matthews, C. S., and C. O. Hurd, *Trans. Am. Inst. Chem. Eng.*, **42**, 55 (1946).
14. Null, H. R., *Chem. Eng. Prog. Symp. Ser. No. (81)*, **63**, 52 (1967).
15. Orye, R. V., and J. M. Prausnitz, *Ind. Eng. Chem.*, **57** (5), 18 (1965).
16. Preston, G. T., and J. M. Prausnitz, paper presented at AIChE, New Orleans meeting (Mar. 17, 1969).
17. Price, A. R., and R. Kobayashi, *J. Chem. Eng. Data*, **4**, (1), 40 (1959).
18. Reid, R. C., and T. K. Sherwood, "The Properties of Liquids and Gases," McGraw-Hill, New York (1958).
19. Rossini, F. D., et al., "Selected Values of Properties of Hydrocarbons and Related Compounds," A. P. I. Res. Proj. 44, Carnegie Inst. Technol. (1958).
20. Wilson, G. M., *J. Am. Chem. Soc.*, **86**, 127 (1964).
21. Wolberg, J. R., "Prediction Analysis," D. Van Nostrand, Princeton (1967).
22. Ziegler, W. T., *Natl. Bur. Std. Tech. Note 4* (May 1959).

Manuscript received June 30, 1969; revision received January 23, 1970; paper accepted January 28, 1970. Paper presented at AIChE Portland meeting.